J Appl Electrochem (2009) 39:1503–1508
DOI 10.1007/s10800-009-9833-2

ORIGINAL PAPER

Effect of heat treatment on PtRu/C catalyst for methanol electro-oxidation

Min Ku Jeon · Ki Rak Lee · Hee Jung Jeon · Seong Ihl Woo

Received: 13 March 2008 / Accepted: 5 February 2009 / Published online: 26 February 2009

Abstract The effect of heat treatment on a commercial PtRu/C catalyst was investigated with a focus on the relationship between electrochemical and surface properties. The heat treated PtRu/C catalysts were prepared by reducing the commercial PtRu/C catalyst at 300, 500, and 600 °C under hydrogen flow. The maximum mass activity for the methanol electro-oxidation reaction (MOR) was observed in the catalyst heat treated at 500 °C, while specific activity for the MOR increased with increasing heat treatment temperature. Cyclic voltammetry (CV) results revealed that the heat treatment caused Pt rich surface formation. The increase in surface Pt was confirmed by X-ray photoelectron spectroscopy; the surface (Pt:Ru) ratio of the fresh catalyst (81:19) changed to (87:13) in the 600 °C heat treated catalyst. Quantitative analysis of the Ru oxidation state showed that the ratio of metallic Ru increased with an increase in heat treatment temperature. On the other hand, RuO_xH_y completely reduced at 500 °C and the ratio of RuO_2 slightly decreased with increasing heat treatment temperature.

M. K. Jeon · K. R. Lee · H. J. Jeon · S. I. Woo (✉)
Department of Chemical and Biomolecular Engineering (BK21 Graduate Program) & Center for Ultramicrochemical Process Systems, Korea Advanced Institute of Science and Technology, 373-1, Guseong-dong, Yuseong-gu, Daejeon 305-701, Republic of Korea
e-mail: siwoo@kaist.ac.kr

Present Address:
H. J. Jeon
Catalysis Technologies Lab., Corporate R&D Center, SK Energy, 140-1, Wonchon-dong, Yuseong-gu, Daejeon 305-712, Republic of Korea

Keywords PtRu/C · Methanol electro-oxidation · Electrocatalyst · CO stripping · X-ray photoelectron spectroscopy

1 Introduction

Methanol electro-oxidation reaction (MOR) catalysts are of great interest especially for their application in direct methanol fuel cells (DMFCs). The development of DMFCs is focused on portable power source applications, such as notebook computers, because DMFCs can be fabricated on a much smaller scale than other fuel cells [1]. Use of a liquid fuel, methanol, makes this a special characteristic of DMFCs. However, the use of methanol significantly reduces the activity of Pt catalysts, which is the original MOR catalyst. Intermediate CO poisons the Pt catalyst and causes a rapid drop in performance [1–3]. Incorporation of Ru dramatically enhances resistance to CO poisoning [4–6] in two ways: a mainly bi-functional mechanism [7, 8] and a minor electronic effect [9–11]. Though there were significant improvements in the mechanism study of thin-film PtRu catalysts, much room is still left to be explored in the powder form catalysts because there are too many parameters (such as synthesis method, particle size, degree of alloying, Ru oxidation state, and surface composition) to be considered at the same time.

One approach to achieving higher activity of the PtRu catalyst for the MOR is the use of a small nanometer scale particle size. However, Xiong and Manthiram [12] reported that the maximum mass activity for the MOR was obtained with a particle size of 5.3 nm. In the paper, mass activity decreases with decreasing particle size when the particle size is smaller than 5.3 nm. Smaller particle size corresponds to a larger electrochemical surface area, therefore

the decrease in the mass activity of PtRu catalysts with particle sizes less than 5.3 nm indicates a much larger decrease in specific activity. In addition, this result shows that there is an optimum particle size of the PtRu catalyst for MOR.

Another approach to achieve higher activity is controlling the oxidation state of Ru. Rolison et al. [13] reported that commercial PtRu catalysts are not single-phase materials but mixtures of various oxides of Pt and Ru. Notably, the molar ratio of Ru metal was below 25% in the commercial catalysts, while the remainder was composed of RuO_2 and RuO_xH_y (hydrous oxide). It was shown that RuO_2 is a poor promoter of methanol electro-oxidation [14], and recent reports also showed that RuO_xH_y is more active than the metallic Ru [15–19]. On the other hand, Lu et al. [20] divided Ru (hydrous) oxides (RuO_2 and RuO_xH_y) into reversible and irreversible ones. They claimed that the reversible Ru (hydrous) oxide is beneficial for MOR, while the irreversible one is harmful. These results warrant the study of the particles size effect in catalysts with the same Ru oxidation state ratio, but, synthesis of such catalysts is not realistic. Therefore, it is clear that investigation on the particle size effect should be carried out in combination with the oxidation state study.

In the present study, the effect of heat treatment under a reducing atmosphere on the PtRu/C catalyst was investigated, especially focusing on the relationship between electrochemical and surface properties. Physical and electrochemical properties were analyzed by using X-ray diffraction data (XRD), cyclic voltammetry (CV), CO stripping and MOR activity measurements. Changes in surface (Pt:Ru) ratio and the Ru oxidation state were studied by X-ray photoelectron microscopy (XPS).

2 Experimental

A commercial PtRu/C (60 wt%, Pt:Ru = 1:1 at.%, E-tek, "PtRu-f") was used as a staring material. Heat treatment was performed by sintering the PtRu-f catalyst at temperatures of 300 ("PtRu-300"), 500 ("PtRu-500"), and 600 °C ("PtRu-600"), under flowing H_2/He (10 vol. % H_2) at a rate 100 mL min^{-1} for 3 h.

Electrochemical studies were performed in a three-electrode-type beaker cell equipped with a platinum wire counter electrode, an Ag/AgCl reference electrode (BAS Co., Ltd., MF-2052 RE-5B) and a glassy carbon working electrode (3 mm dia., BAS Co., Ltd., MF-2012). The working electrodes were prepared by the thin-film electrode method [21]. A certain amount of catalyst was dispersed in DI water, followed by sonication. 10 μL of the catalyst dispersion was then dripped on the working electrode. After drying at room temperature, 5 wt% Nafion ionomer solution was dripped on the working electrode to stabilize the catalyst layer. All potentials shown in this paper are converted to the reference hydrogen electrode (RHE) scale. The CV experiments were carried out in N_2 purged 1 M $HClO_4$ solution by potential cycling between 0 and 1.4 V at a scan rate of 15 mV s^{-1}. For the CO stripping tests, CO was adsorbed on the catalyst surface by bubbling CO through the cell for 1 h while keeping the working electrode potential at 0.1 V. Excess CO was removed by purging N_2 through the cell for 50 min. CO stripping was then measured by increasing the potential to 1.2 V at a scan rate of 15 mV s^{-1}. Nitrogen purged 1 M $HClO_4$ solution was used as the electrolyte. The MOR activity measurement was performed in N_2 purged 1 M H_2SO_4 + 1 M methanol solution by potential cycling between 0 and 0.8 V at a scan rate of 15 mV s^{-1}. All electrochemical experiments were conducted at 25 °C.

3 Results and discussion

Figure 1 shows the XRD measurement results of (a) the fresh PtRu/C catalyst (PtRu-f) and the catalysts sintered at (b) 300 (PtRu-300), (c) 500 (PtRu-500), and (d) 600 (PtRu-600), respectively. The particle size as a function of the heat treatment temperature was calculated from the full-width at half maximum of the (111) peak near 40° by using the Debye-Scherrer equation [22]. The particle size increased from 3.1 nm in the PtRu-f to 4.3, 5.9, and 8.5 nm in the PtRu-300, PtRu-500, and PtRu-600 catalysts, respectively. In addition, the (111) peak from 40.23° in the PtRu-f catalyst moved to higher 2θ values of 40.36, 40.41, and 40.42° in the PtRu-300, PtRu-500, and PtRu-600 catalysts, respectively. This peak shift indicates that a higher degree of alloying was achieved by increasing the heat

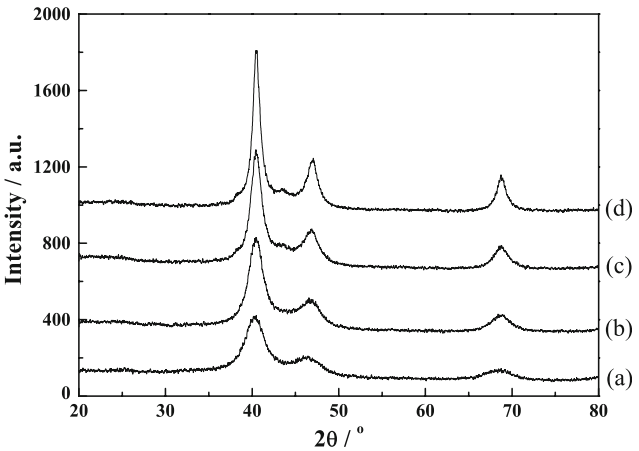

Fig. 1 XRD patterns of (a) PtRu-f, (b) PtRu-300, (c) PtRu-500, and (d) PtRu-600

Table 1 Summary of the XRD results

	(111) Peak position (°)	d (nm)	Lattice parameter (nm)	Particle size (nm)
PtRu-f	40.23	0.2240	0.3880	3.1
PtRu-300	40.36	0.2233	0.3868	4.3
PtRu-500	40.41	0.2231	0.3864	5.9
PtRu-600	40.42	0.2230	0.3862	8.5

treatment temperature. A summary of the XRD results are shown in Table 1.

The CO stripping results are shown in Fig. 2. The electrochemically active surface area (EAS) was calculated from the CO stripping area, which decreased from 26 m^2 g_{catal}^{-1} in the PtRu-f catalyst to 15, 13, and 7.1 m^2 g_{catal}^{-1} in the PtRu-300, PtRu-500, and PtRu-600 catalysts, respectively. This result was caused by the increase in particle size as noted in the XRD results. Peak potential for CO electro-oxidation was also varied with the heat treatment temperatures. The peak potential decreased from 0.55 V in the PtRu-f catalyst to 0.52 V in the PtRu-300 catalyst. When the heat treatment temperature was further increased to 500 and 600 °C, the peak potential increased to 0.54 and 0.55 V. The CO stripping results are discussed in detail at the end of this section.

The MOR activity measurement results are shown in Fig. 3. Measured current densities at 0.7 V were 14.8, 30.3, 32.0, and 22.7 mA cm^{-2} for the PtRu-f, PtRu-300, PtRu-500, and PtRu-600 catalysts, respectively. The mass and specific activities are listed in Table 2. The mass activity plot with respect to the particle size showed a volcano shape which exhibited the highest mass activity in the PtRu-500 catalyst (5.9 nm). On the other hand, with increasing heat treatment temperature, the specific activity significantly increased from 0.50 A m^{-2} in the PtRu-f catalyst to 1.8, 2.2, and 2.8 A m^{-2} in the PtRu-300, PtRu-500, and PtRu-600 catalysts, respectively. Li et al. [23] and

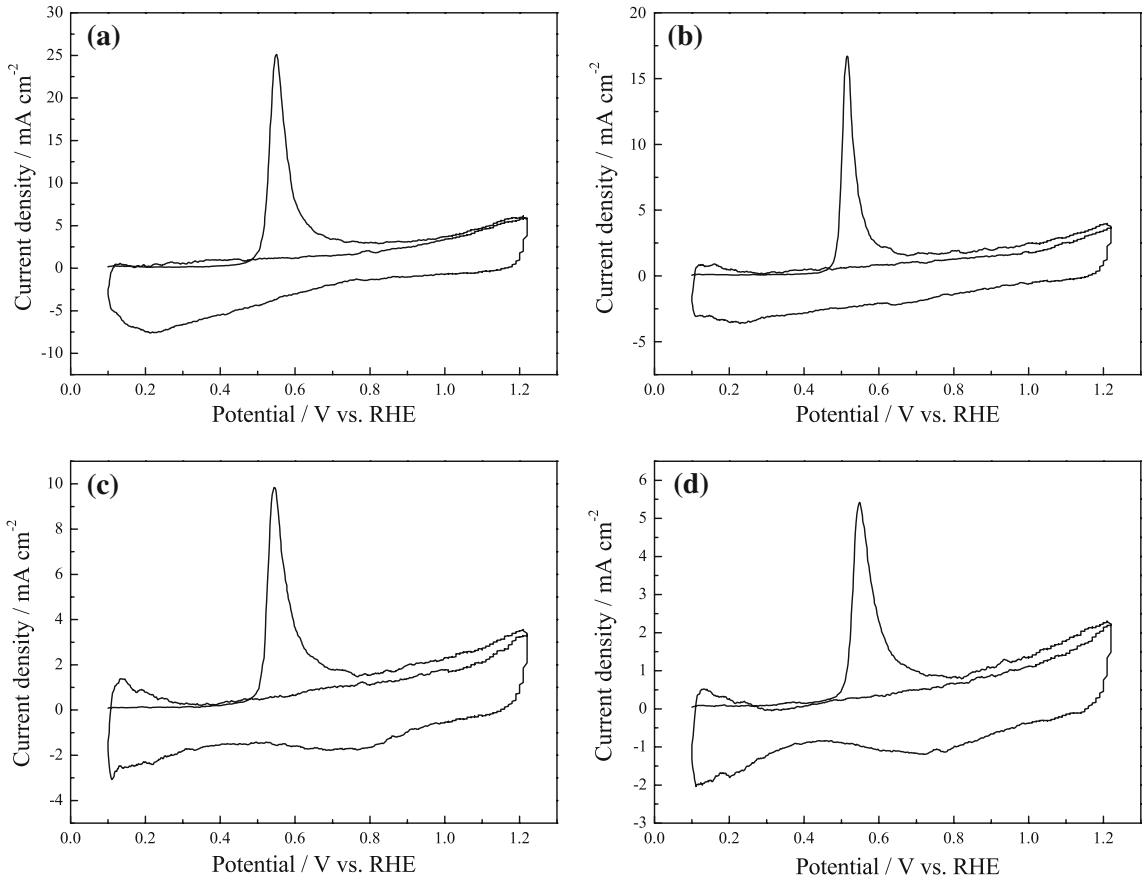

Fig. 2 CO stripping results of **a** PtRu-f, **b** PtRu-300, **c** PtRu-500, and **d** PtRu-600. 1 M $HClO_4$ solution was used as the electrolyte and scan rate was 15 mV s^{-1}

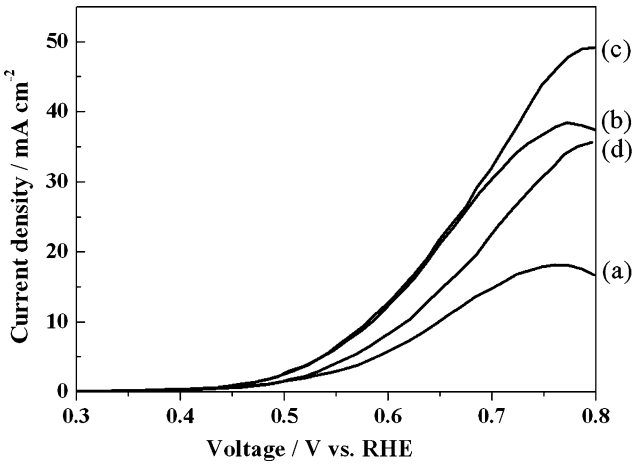

Fig. 3 Methanol electro-oxidation activity of (a) PtRu-f, (b) PtRu-300, (c) PtRu-500, and (d) PtRu-600. 1 M H_2SO_4 + 1 M methanol solution was used as the electrolyte and scan rate was 15 mV s^{-1}

Takasu et al. [24] also reported that heat treatment can increase specific activity of the PtRu catalyst. This behavior can be explained by Pt rich surface formation during the heat treatments under reducing atmosphere due to Pt–H interactions [25–27].

Figure 4 shows the CV results of the PtRu/C catalysts measured for 30 cycles. Changes according to the number of cycles are denoted by arrows. The increase in current density above 0.4 V (along the positive scan direction) and below 0.6 V (along the negative scan direction) comes from oxidation/reduction of the irreversible Ru (hydrous) oxides. The current density from the irreversible Ru (hydrous) oxides decreased with increasing number of CV cycles, which means dissolution or formation of reversible Ru (hydrous) oxides. A lack of noticeable changes in the proton adsorption region (0 ~ 0.3 V along the positive scan direction) indicates that the irreversible Ru (hydrous) oxides were changed to the reversible Ru (hydrous) oxides during the CV tests [20]. In the heat treated catalysts, oxidation/reduction of the irreversible Ru (hydrous) oxides was also observed; however, a change in the current density corresponding to the increasing number of CV cycles was significantly suppressed. This result means a more stable surface was formed by a higher degree of alloying and Pt rich surface formation. One point to be noted is the shift of PtO reduction peak which was near 0.4 V in the PtRu-f catalyst and moved to higher potentials to reach 0.63 V in the PtRu-600 catalyst. Pure Pt has the reduction peak near 0.72 V [28], which means more Pt-like surface was formed by the higher heat treatment temperature. This result is in accordance with the above results, which suggested that Pt rich surface formation occurred during the heat treatments. The formation of a Pt rich surface appears to be contradictory to the XRD results, which showed a higher degree of alloying with higher heat treatment temperatures. But, it can be resolved by realizing that, though a higher degree of alloying was achieved in the bulk by high temperature treatment, the surface property was changed to Pt rich phase. The MOR activity and CV results could provide only qualitative information. For quantitative analysis of surface composition and Ru oxidation state, XPS measurements were performed.

Surface composition analysis results are shown in Table 2, and they prove the formation of a Pt rich surface and an increase in the ratio of Pt with increasing heat treatment temperature. However, the (Pt:Ru) ratio between the PtRu-500 and PtRu-600 were identical (87:13), indicating that this ratio is a saturation point under the reducing atmosphere used in this study. The increase in Pt ratio explains the increase of specific activity caused by the heat treatments. Previously Dickinson et al. [29] reported that a 3:2 ratio of Pt:Ru yields a higher MOR activity than 1:1 at 25 °C, while it is reversed at 65 °C. Alternatively, Gasteiger et al. [30] reported that 10 at.% Ru is the optimum surface ratio at 25 °C. In our results, the surface ratio of Ru was 19 at.% though that of bulk was 50 at.%. This result explains the differing composition results in the two reports and the increase of the specific activity by the formation of Pt rich surface which was observed in this paper. Study of the thin-film type PtRu catalysts also supports this result in their observation of the best composition in 10 ~ 20 at.% Ru ratio region [6, 7, 31, 32].

The deconvoluted results of the XPS data on Ru are shown in Fig. 5. Metallic Ru, RuO_2 and RuO_xH_y were assigned at 280.1, 280.9, and 282 eV, respectively. The molar ratio of each oxidation state is listed in Table 2. The

Table 2 Summary of the electrochemical properties and surface analysis results

	EAS from CO (m^2 g_{catal}^{-1})	EAS per electrode surface area	Current density at 0.7 V (mA cm^{-2})	Mass activity (A g_{catal}^{-1})	Specific activity (A m^{-2})	Ru:RuO_2: RuO_xH_y molar ratio	Pt:Ru surface composition determined by XPS (at.%)
PtRu-f	26	2.9	14.8	13.0	0.50	6:62:31	81:19
PtRu-300	15	1.7	30.3	26.5	1.8	19:69:12	82:18
PtRu-500	13	1.5	32.0	28.0	2.2	70:30:0	87:13
PtRu-600	7.1	0.80	22.7	19.9	2.8	74:26:0	87:13

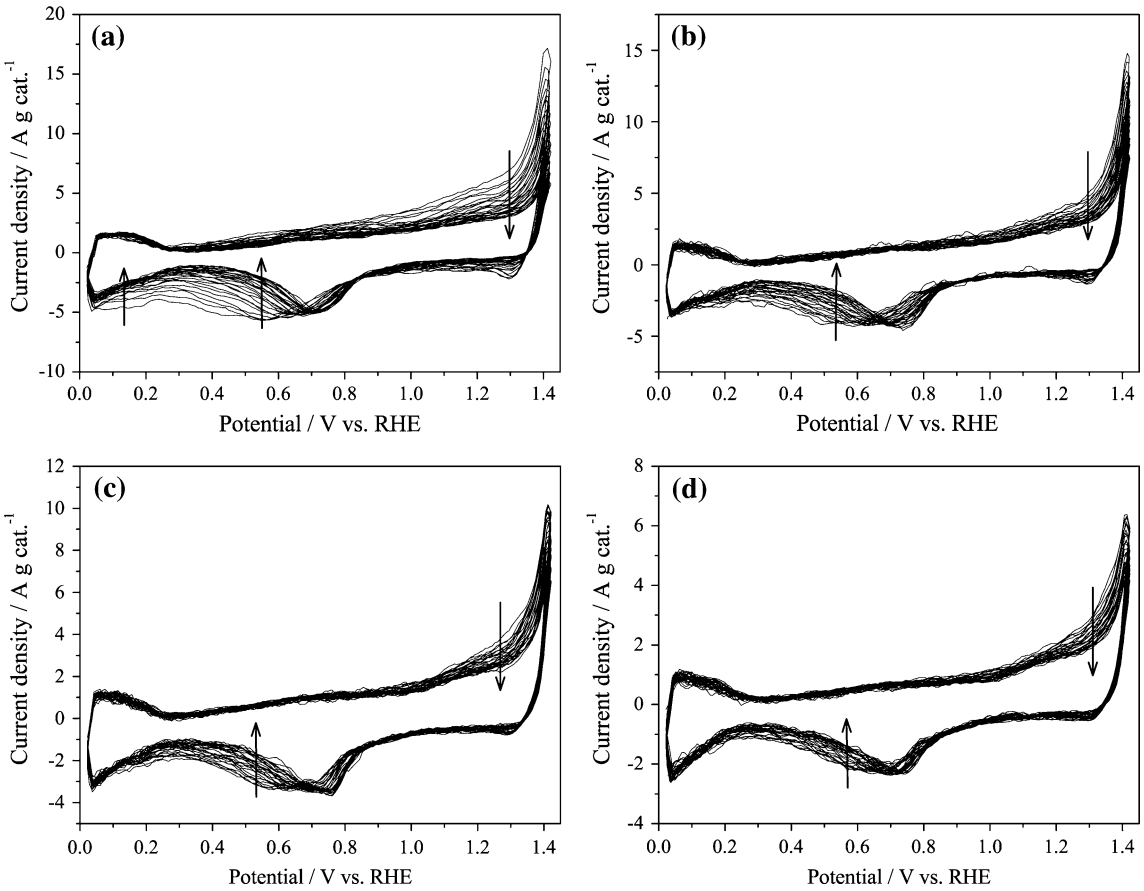

Fig. 4 Cyclic voltammetry results of the **a** PtRu-f, **b** PtRu-300, **c** PtRu-500, and **d** PtRu-600 catalysts. 1 M $HClO_4$ solution was used as the electrolyte. CV was measured by potential cycling between 0 and 1.4 V (vs. RHE) at a scan rate of 15 mV s^{-1}

PtRu-f catalyst had a ($Ru:RuO_2:RuO_xH_y$) ratio of (6:62:31) while the ratio changed to (19:69:12) in the PtRu-300 catalyst. Here, the ratio of RuO_xH_y decreased to less than half, while that of the metallic Ru increased. The increase in the RuO_2 amount may have resulted from an experimental error. In the PtRu-500 catalyst, the RuO_xH_y species was completely reduced to the metallic Ru. The reduction of RuO_xH_y does not account for the improved MOR specific activities in the PtRu-300 and PtRu-500 catalysts, because it has been reported that RuO_xH_y has higher activity than Ru as noted above. This result means other parameters (degree of alloying, particle size, Pt rich surface formation, and reversible Ru (hydrous) oxide formation) could improve the MOR specific activity in spite of the loss of RuO_xH_y. But the specific cause is not clear, since all of the parameters were changed at the same time. In the PtRu-500 and PtRu-600 catalysts, there were no changes of the (Pt:Ru) ratio. However, the ratio of metallic Ru increased from 70% in the PtRu-500 catalyst to 74% in the PtRu-600 catalyst. Though only 4% of RuO_2 was reduced to metallic Ru, the specific activity of the PtRu-600 catalyst increased 27%, which might be due to the larger particle size of the PtRu-600 catalyst.

Discussion on the CO stripping results should be further mentioned at this point. Previously Maillard et al. [33] reported that the lowest CO electro-oxidation peak potential was obtained with a Pt particle size of 3.3 nm, and Camara et al. [34] showed that the best CO tolerance was achieved when Pt:Ru alloy real proportion was 3:1. Therefore, the CO electro-oxidation reaction is a function of both the particle size and surface composition. In our results, the best CO electro-oxidation was observed in PtRu-300, while PtRu-600 exhibited the highest specific activity for the MOR, indicating that the optimum condition for each (CO and methanol) reactions is different. A more detailed study on this issue is desirable to clarify this difference.

4 Conclusions

The effect of heat treatment under a reducing atmosphere was investigated with a focus on the relationship between the electrochemical and surface properties. In the MOR, the specific activity increased with increasing heat treatment temperature, and the PtRu-500 catalyst exhibited the

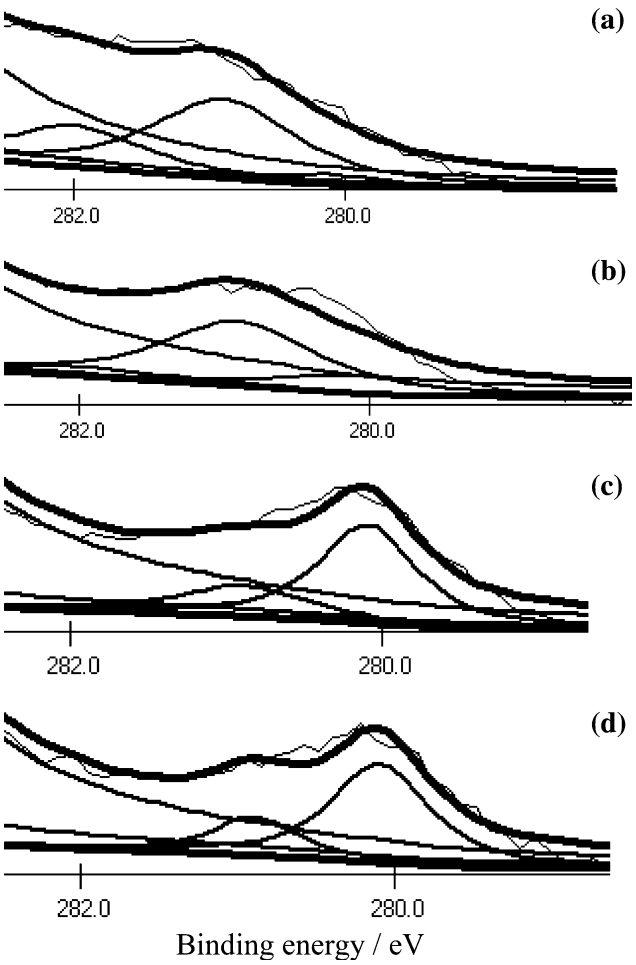

Fig. 5 Ru_3d XPS results of the **a** PtRu-f, **b** PtRu-300, **c** PtRu-500, and **d** PtRu-600 catalysts. Axes are: the *x*-axis is binding energy (eV) and the *y*-axis is intensity (a.u.)

highest mass activity as a trade-off point between the decrease in the surface area and the increase in the specific activity. The CV results showed that a Pt rich surface was formed by the heat treatments, which was confirmed by the XPS results. In the oxidation state of Ru, it was observed that the most active RuO_xH_y was completely reduced when heat treated at 500 °C, but changes in other parameters could increase the specific activity of the PtRu-500 and PtRu-600 catalysts.

Acknowledgments This research was partially funded by the Center for Ultramicrochemical Process Systems (CUPS) sponsored by KOSEF (2008). The authors also thank Research Park/LG Chem, Ltd. and Ministry of Commerce, Industry and Energy for funding this research in the framework of the Korean government/industry joint project for the development of 50 W direct methanol fuel cell systems.

References

1. Arico AS, Srinivasan S, Antonucci V (2001) Fuel Cells 1:133
2. Thomas SC, Ren X, Gottesfeld S, Zelenay P (2002) Electrochim Acta 47:3741
3. Petrii OA (2008) J Solid State Electrochem 12:609
4. Watanabe M, Motoo S (1975) J Electroanal Chem 60:267
5. Markovic NM, Gasteiger HA, Ross PN Jr (1995) Electrochim Acta 40:91
6. Chrzanowski W, Wieckowski A (1998) Langmuir 14:1967
7. Gasteiger HA, Markovic N, Ross PN, Cairns EJ (1993) J Phys Chem 93:12020
8. Yajima T, Uchida H, Watanabe M (2004) J Phys Chem B 108:2654
9. Rodriguez JA, Goodman DW (1992) Science 257:897
10. Kitchin JR, Nørskov JK, Barteau MA, Chen JG (2004) Phys Rev Lett 93:156801
11. Rigsby MA, Zhou WP, Lewera A, Duong HT, Bagus PS, Jaegermann W, Hunger R, Wieckowski A (2008) J Phys Chem C 112:15595
12. Xiong L, Manthiram A (2005) Solid State Ion 176:385
13. Rolison DR, Hagans PL, Swider KE, Long JW (1999) Langmuir 15:774
14. Kennedy BJ, Smith AW (1990) J Electroanal Chem 293:103
15. Long JW, Stroud RM, Swider-Lyons KE, Rolison DR (2000) J Phys Chem B 104:9772
16. Jeon MK, Won JY, Woo SI (2007) Electrochem Solid-State Lett 10:B23
17. Gavrilov AN, Savinova ER, Simonov PA, Zaikovskii VI, Cherepanova SV, Tsirlina GA, Parmon VN (2007) Phys Chem Chem Phys 9:5476
18. Lasch K, Jörissen L, Friedrich KA, Garche J (2003) J Solid State Electrochem 7:619
19. Rose A, Crabb EM, Qian Y, Ravikumar MK, Wells PP, Wiltshire RJK, Yao J, Bilsborrow R, Mosselmans F, Russell AE (2007) Electrochim Acta 52:5556
20. Lu Q, Yang B, Zhuang L, Lu J (2005) J Phys Chem B 109:1715
21. Schmidt TJ, Gasteiger HA, Stäb GD, Urban PM, Kolb DM, Behm RJ (1998) J Electrochem Soc 145:2354
22. He CZ, Kunz HR, Fenton JM (1997) J Electrochem Soc 144:970
23. Li X, Hsing IM (2006) Electrochim Acta 52:1358
24. Takasu BY, Itaya H, Iwazaki T, Miyoshi R, Ohnuma T, Sugimoto W, Murakami Y (2001) Chem Commun 4:341
25. Schmidt TJ, Noeske M, Gasteiger HA, Behm RJ, Britz P, Bönnemann H (1998) J Electrochem Soc 145:925
26. McNicol BD, Short RT (1977) J Electroanal Chem 81:249
27. Hwang BJ, Sarma LS, Wang GR, Chen CH, Liu DG, Sheu HS, Lee JF (2007) Chem Eur J 13:6255
28. Jeon MK, Daimon H, Lee KR, Nakahara A, Woo SI (2007) Electrochem Commun 9:2692
29. Dickinson AJ, Carrette LPL, Collins JA, Friedrich KA, Stimming U (2004) J Appl Electrochem 34:975
30. Gasteiger HA, Markovic N, Ross PN Jr, Cairns EJ (1994) J Electrochem Soc 141:1795
31. Cooper JS, McGinn PJ (2006) J Power Sources 163:330
32. Whitacre JF, Valdez T, Narayanan SR (2005) J Electrochem Soc 152:A1780
33. Maillard F, Schreier S, Hanzlik M, Savinova ER, Weinkauf S, Stimming U (2005) Phys Chem Chem Phys 7:385
34. Camara GA, Giz MJ, Paganin VA, Ticianelli EA (2002) J Electroanal Chem 537:21